Internal flow and air core dynamics in Simplex and Spill-return pressure-swirl atomizers

MALÝ, M.; JEDELSKÝ, J.; SLÁMA, J.; JANÁČKOVÁ, L.; SAPÍK, M.; WIGLEY, G.; JÍCHA, M.

International journal of heat and mass transfer
2018, vol. 123, August 2018, pp. 805-814

ISSN: 0017-9310

DOI: https://doi.org/10.1016/j.ijheatmasstransfer.2018.02.090

Accepted manuscript

Internal flow and air core dynamics in Simplex and Spill-return pressure-swirl atomizers

Milan Malý*[1], Jan Jedelský[1], Jaroslav Sláma[2], Lada Janáčková[1], Marcel Sapík[1], Graham Wigley[3], Miroslav Jícha[1]

[1] Faculty of Mechanical Engineering, Brno University of Technology, Czech Republic

[2] Provyko s.r.o, Czech Republic

[3] Loughborough University, United Kingdom

*Corresponding author: milan.maly@vutbr.cz

Abstract

Spill-return (SR) atomizers enhance the construction of Simplex atomizers by addition of a passage in the rear wall of the swirl chamber through which the liquid can be spilled away. It allows to discharge the liquid always at a high pressure and to spray well over a wide flow rate range. The spray characteristics of pressure-swirl atomizers are strongly linked to the internal flow, and the air-core dynamics affect the spray stability. The SR atomizers are rarely studied and their internal flow is not studied at all. Therefore, in this paper, the Simplex and SR atomizers with a central SR orifice were examined comparatively.

Transparent polymethyl methacrylate (PMMA) models of both atomizers scaled 10:1 were manufactured for the visualization and velocity measurements of the flow inside the swirl chamber. The atomizers were examined by means of high-speed imaging, laser-Doppler anemometry and computational fluid dynamics tools. The experimental and numerical results were analysed and compared in terms of the spray cone angle (SCA), discharge coefficient (C_D), and the morphology and temporal stability of the air core. The internal flow characteristics between the original and the model were matched using the Reynolds, Swirl and Froude numbers. The test conditions were limited to inlet Reynolds numbers from 750 to 1750.

The results show that the addition of the spill passage strongly affects the internal flow even if the spill-line is closed. The air core in the Simplex atomizer is fully developed and stable for all flow regimes. The SR atomizer behaved differently; with closed spill-line (spill-to-feed ratio, SFR=0), the air core does not form at all; therefore the spray is unstable. The reason is that the liquid, contained in the spill-line, is drained back into the swirl chamber due to a recirculation zone found inside the spill-line. Increasing the SFR stabilizes the internal flow, and the spray becomes stable if SFR > 0.15. The air core begins to form for SFR > 0.4. The results suggest that the axially positioned spill orifice is inappropriate and its placing off-axis would improve the spray stability. The results of the 2D numerical simulation matched closely with the experiments in terms of SCA, C_D, velocity profiles, and air core morphology which proved its prediction capabilities.

Keywords

Internal flow dynamics, Pressure-swirl, transparent nozzle, CFD

1 Introduction

Pressure-swirl (PS) atomizers are used in many applications where a large surface area of droplets is needed, or a surface must be coated with a liquid, e.g. combustion, fire suspension or air conditioning. PS atomizers are easy to manufacture, reliable and provide good atomization quality. They convert the pressure energy of the pumped liquid into kinetic and surface energy of the resulting droplets. The liquid is injected via tangential ports into a swirl chamber where it gains a swirl motion under which it leaves the exit orifice as a conical liquid sheet. The centrifugal motion of the swirling liquid creates a low-pressure zone in the centre of the swirl chamber and generates an air core along the centreline. The flow inside the atomizer is rather complex; it is two-phase with secondary flow effects. There is a strong link between internal flow conditions and the resulting spray characteristics. However, not all aspects of the internal flow are well understood. A drawback of the Simplex atomizer is that the droplet size depends on the inlet pressure, hence on the liquid flow rate. The flow rate varies as the square root of the injection pressure. Thus, doubling the flow rate demands a fourfold increase in injection pressure, which means that the range of applicable flow rates is limited and thus the turn-down ratio (defined as ratio of

maximum liquid flow rate to minimum liquid flow rate which fulfils the requirement of atomization quality) is usually low [1]. This disadvantage can be eliminated using a SR atomizer which is basically a Simplex type with a passage added in the rear wall of the swirl chamber, see Figure 1. When the spill-line is closed, the atomizer operates as a standard Simplex type. When a low injection flow rate is required, the liquid is spilled away through the spill orifice while the inlet pressure and the swirl momentum remain high, and the atomization quality remains. However, increasing spilled flow rate causes reduction in the axial momentum of discharged liquid which consequently leads to change in the spray cone angle (SCA), as the SCA is determined by the ratio of the swirl momentum to the axial momentum. Another drawback is the requirement for increased pump power and complicated for flow metering. For these reasons, the interest in SR atomizers for aircraft combustors declined, however, if the aromatic content of gas turbine fuels rises, gum formation in the small sized atomizers could pose serious problems of the atomizer blockage [2, 3]. The SR atomizers are virtually free of this defect as they have no small passages. Beside the aircraft combustors, the SR atomizer were used in stationary gas turbines [4] and industrial burners [5]. However, the above-mentioned advantages of SR atomizers are crucial in special applications that require a fine spray at very low flow rate, e.g. decontamination devices [6], or for atomization of waste fuels and liquids containing impurities where large dimensions of flow cross-sections are necessary to prevent the atomizer from clogging, or in applications where pneumatic atomizers are not allowed but the wide regulation range is required. The studied spill-return atomizer is originally used in a combustion chamber of small turbojet aircraft engine manufactured by PBS Velká Bíteš, a.s., Czech Republic.

Before the advent of computational fluid dynamics, a number of authors attempted to describe the internal flow of Simplex atomizer by relatively simple analytical approaches. One of the first was presented by Taylor [7] who focused on an inviscid analysis using Bernoulli's equation and the principle of maximal flow. Taylor derived an equation for the discharge coefficient (C_D) and the spray cone angle (SCA) solely dependent on the atomizer constant $k = 2 \cdot A_p/(\pi \cdot d_o \cdot d_s)$, where A_p is the total area of the inlet ports, d_o, and d_s are defined in Figure 1. Similar results were found independently by other authors, and these works have been compared and reviewed by Chinn [8, 9]. Results obtained by the inviscid theory are not generally in good agreement with experiments. However, findings from the inviscid theory may be used as a basis for design improvements.

The experimental correlations for C_D were found to be more complex than the inviscid theory predicted. Rizk and Lefebvre [10] derived a semi-empirical correlation where, besides the constant k, the ratio d_s/d_o had a strong influence. Jones [11] found a weak dependence of C_D on the length of the swirl chamber and exit orifice, and liquid viscosity. Ballester [12] added a dependence on the inlet pressure. Benjamin [13] followed the work of Jones [11] and found inverse trends for some parameters. Wimmer and Brenn [14] theoretically uncovered a relatively strong effect of the liquid viscosity on C_D, which was later experimentally confirmed by Maly et al. [15].

The internal flow characteristics, especially the air core stability, were investigated by a few authors. Halder [16] investigated the air core shape in 21 different transparent atomizers at various inlet mass flow rates of water. Two limiting values of Reynolds number (*Re*) were conducted for the inception of the air core for each atomizer. Below the lower limit, the air core was not formed at all, while above the upper limit, it was always found to be stable. He observed that the limiting *Re* decreases with an increase in d_o/d_s and a decrease in A_p/d_s. The stable air core had a cylindrical shape, and for large *Re* values, it was almost constant in diameter. For *Re* values close to the limiting value, the diameter of the air core increased sharply with increasing *Re*. A similar concept of limiting values of *Re* was introduced by Lee et al. [17]. In this experimental work, a transparent atomizer with diesel and kerosene used over a range of inlet pressures and temperatures. They deduced that the air core stability was a function of *Re* related to the exit orifice, Re_o. It was stable for $Re > 3300$; at lower values it became unstable until for Re_o below 2400, where there was no air core at all due to insufficient centrifugal forces, and the spray fluctuated strongly. Kim et al. [18] investigated the influence of diameter and length of the swirl chamber on the air core stability. Atomizers with a ratio of swirl chamber height to its diameter h_s/d_s higher than 1.27 demonstrated an unstable air core. The authors [18] described the unstable air core as having a rotating and double helical structure. Moon [19] found a limiting value of the swirl number $S_0 = 0.6$, which ensured a stable air core. The same limiting value of S_0 was also proposed by Park [20] for swirling jets.

SR atomizers have rarely been studied, and their internal flow has not been documented so far to the best of our knowledge. Especially the effect of the spill orifice arrangement on the internal flow is

not at all clear. The liquid spill can be realized by a single axial orifice, by several off-axis orifices, or by an annular slot [21]. The simplest designs use a single, axially placed spill orifice but the problems with spray stability were reported [21-23], especially under operating regimes with a closed spill-line.

The former approaches to study the internal flow were mostly experimental [24, 25] and analytical [8, 9, 26]. The application of CFD has greatly simplified design process of the atomizer due to increase in computing performance in recent years. In 1997, Yule and Chinn [27] conducted one of the first numerical studies using a 2D simulation. They assumed a laminar flow even for *Re* = 50,000; an internal air-core was captured by the Volume of Fluid (VOF) method. They reported the difference between numerical calculations and the experiment to be less than 3%. Similarly a 2D laminar setup was used by Amini [28] and Mandal [29]; both authors reported a close match with experimental data. Summer [30] compared 2D and 3D simulations with a laminar solution and found only a small differences between them. Madsen [31] tested laminar and turbulent k-ε models together with a Large Eddy Simulation (LES). The turbulent model overestimated the turbulent viscosity; the air-core was not formed at all. The laminar model was comparable to the LES predictions. Various models to capture the liquid–air interface were investigated by Baharanchi [32]. A geometrical reconstruction scheme was found to be an optimal method for capturing the air core. While there are some papers providing CFD simulations of Simplex atomizers, no numerical simulation of SR atomizer were found.

Due to the lack of published results on SR atomization, the present study investigated experimentally and numerically the internal flow of SR atomizer. Firstly the work examines the possibility to predict the atomizer characteristics such as C_D and SCA, and the velocity field in the swirl chamber, using a relatively simple 2D simulation. The main focus is to elucidate on the spray fluctuations, reported in our previous works [22, 33], and to determine their source. Furthermore, the internal flow characteristics are to be compared with a Simplex atomizer.

2 Atomizer geometries and liquid properties

The experiments were performed using both Simplex and SR atomizer designs. In order to examine the internal flow, the atomizers were manufactured as transparent copies. Due to the small dimensions of the original atomizers (see Figure 1), it was impossible to manufacture them and to examine their flows directly. To solve this issue, the transparent versions were designed as ten times scaled copies. The scaled atomizers have a modular construction (Figure 2, right). The assembly consists of three parts, each made from PMMA. The bottom part contains the swirl chamber with the exit orifice, the central one forms the tangential inlet ports, while the top part is a plain wall, in the case of Simplex atomizer or, contains the spill orifice in the case of the SR atomizer. This modular construction allows for each part to be replaced by another one of a different geometry or shape. The surfaces of each part were ground and polished to achieve the transparency sufficient for optical access.

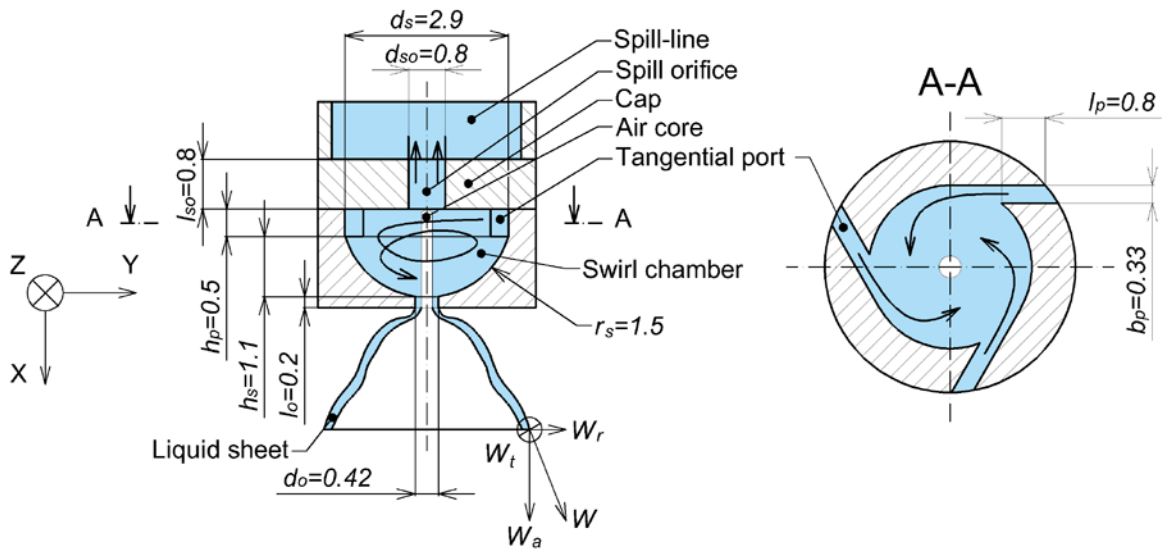

Figure 1. A sketch of the original SR atomizer with the main dimensions in millimetres. The Simplex atomizer has the same geometry and size, but the spill-line orifice is missing. The transparent atomizer has the same shape, and all dimensions are 10 times larger.

Due to the ten times model scale it is necessary to match the flow of the original and scaled atomizers so the relevant dimensionless numbers must be considered. *Re* is defined as the ratio of inertial force to the viscous force. In the case of the swirl atomizer, the most common definition of *Re* is related to the inlet ports [34] as:

$$Re = w_p d_p / \nu \tag{1}$$

where w_p is the mean velocity in the inlet ports, calculated as a volumetric flow rate divided by the total cross-section of inlet ports, ν is the liquid kinematic viscosity, and d_p is the hydraulic diameter of the inlet ports:

$$d_p = 2h_p b_p / (h_p + b_p) \tag{2}$$

, for dimensions, see figure 1. The *Re* values for the scaled model must match those of the original to keep the same internal flow character. The Swirl number S_0 is useful in determining the ratio of the angular momentum to the axial momentum. It can be calculated as a function of the internal geometry [34]:

$$S_0 = \pi R\ r_0 / A_p \tag{3}$$

where R is a radius of flow entry to the swirl chamber and A_p is the total cross-section of the inlet ports. It is obvious that the swirl numbers for the original and scaled atomizers are identical. The Froude number (*Fr*) shows the effect of gravity in comparison with the energy of the bulk flow and is calculated as:

$$Fr = \frac{Q}{2\pi(r_o^2 - r_{oa}^2)\sqrt{r_o g}} \tag{4}$$

where Q is the volume flow rate and r_{oa} is the radius of the air core in the exit orifice. To minimize the effect of gravity, it is necessary to keep $Fr >> 1$, as in the original atomizer case. The Froude number for the lowest pressure used was 6.9 thus the effect of the gravity was small. Spray related dimensionless numbers, such as Weber number and Ohnesorge number differ between the original and scaled atomizers by an order of magnitude thus the spray parameters were not investigated except for the spray cone angle, SCA, close to the exit orifice.

Table 1 lists the experimental flow regimes with their dimensionless numbers. The operating regimes were derived from those used in previous study [22]. The main control parameter was the inlet pressure of the original atomizers and consequently its mass flow rate, from which the *Re* was calculated. The SR atomizer was evaluated with both the closed spill-line to simulate the maximum injection rate and various spill-to-feed (SFR) regimes. Kerosene-type Jet A-1 representing the commonly used fuel was used in both the original and modelled atomizer. However, the refractive index of kerosene differs from the refractive index of the PMMA by about 0.05 at 660 nm wavelength at 25 °C which disturbs the optical measurement close to the internal surfaces of the transparent model. A liquid with a refractive index very close to the PMMA should be used to reduce the optical distortions. For this purpose, several different liquids and mixtures were evaluated to determine the most suitable. Paracymene (p-cymene or 1-Methyl-4-(propan-2-yl)benzene) was chosen. It is a colourless, transparent organic compound with a refractive index different from Plexiglas by less than 0.001 at 660 nm wavelength and at 25 °C. It also has a relatively low aggressiveness to PMMA; however, after a few hours of measurement, it did cause cracks in those parts where increased internal stresses may be anticipated, i.e. in the vicinity of bolts and threads; thus, it was only used for high-speed imaging. The physical properties of Jet A-1 are $\sigma = 0.029$ kg/s^2, $\mu_l = 0.0016$ kg/(m·s), $\rho_l = 795$ kg/m^3 and p-cymene: $\sigma = 0.028$ kg/s^2, $\mu_l = 8\times10^{-4}$ kg/(m·s), $\rho_l = 850$ kg/m^3.

Similarly designed test benches were used for testing of both the original and scaled atomizers, see Figure 2. The test liquids were supplied to the atomizer (8) from a fuel tank (1) via a filter (2) by a gear pump or a centrifugal pump (3) for the original and the scaled atomizer respectively. The mass flow was regulated by varying the pump speed. The fuel flowing through the inlet line was metered by the Coriolis mass flow meter Mass 2100 Di3 fitted with the Mass 6000 transmitter (Siemens AG, GE) (4)

with an accuracy ±0.1% of the actual flow rate. Static inlet over-pressure was measured by a piezo-resistive pressure sensor DMP 331i (BD SENSORS s.r.o., CZ) (7). The uncertainty in the pressure sensing was 0.05 kPa and 2 kPa for the scaled and the original atomizer respectively as different sensors were used in each case. The inlet line was also equipped with a temperature sensor PR-13 made by OMEGA Engineering, INC., USA with an error of 0.2 °C. The spill-line had a piezo-resistive pressure sensor DMP 331i (BD SENSORS s.r.o., CZ) (9), a ball valve (11) and a positive displacement flow meter KOBOLD DOM-S05 with accuracy ±1% of the actual flow rate (KOBOLD Messring GmbH, GE) (10). The calculated uncertainty of C_D at Re = 1021was 0.14 % and 0.25 % for original and scaled Simplex atomizer respectively. The atomized liquid was captured by a collection chamber and routed back into the fuel tank. Fuel mist and vapours were ventilated by a fan. The atomizer was mounted to a CNC positioning system with a positional error less than 0.1 mm.

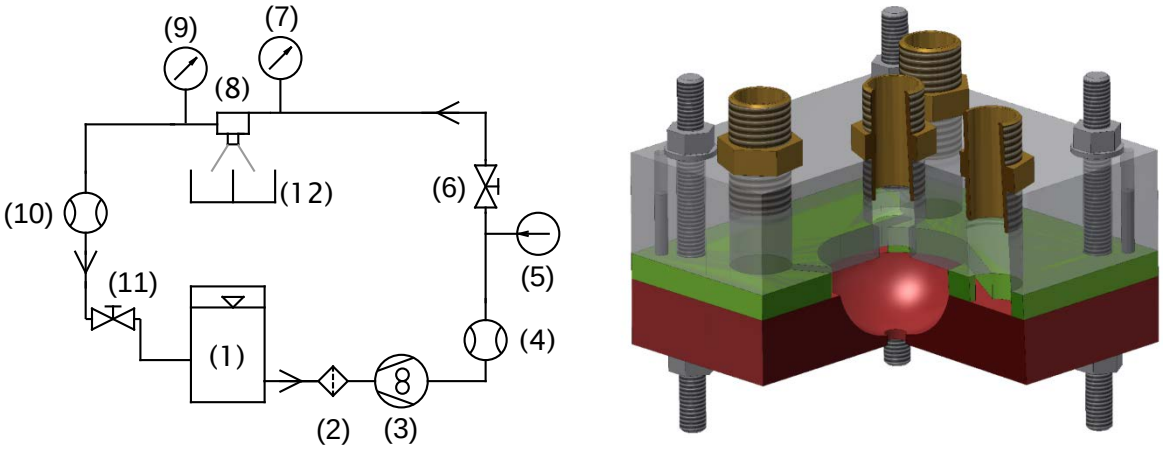

Figure 2 Left: Schematic layout of liquid supply. Right: A Schematic of the scaled transparent atomizer

Table 1 Operating flow regimes, kerosene, S_0 = 3.87

		Original atomizer				Scaled atomizer			
	Re	***Δp***	m_l	C_D	***Fr***	***Δp***	m_l	C_D	***Fr***
	[–]	**[MPa]**	**[kg/h]**	**[–]**	**[–]**	**[kPa]**	**[kg/h]**	**[–]**	**[–]**
Simplex	755	0.5	5.41	0.387	137	5	53.8	0.378	6.9
Simplex	1021	1	7.31	0.369	293	10	73.1	0.366	9.3
Simplex	1252	1.5	8.97	0.365	359	15	88.2	0.362	11.4
SR	1075	0.5	7.7	0.542	308	5	69.4	0.483	9.8
SR	1431	1	10.25	0.519	411	10	93.4	0.466	13.0
SR	1731	1.5	12.4	0.510	497	15	110.0	0.454	15.7
SR, SFR 0.4	1676	1	12.0	0.378	481	10	103	0.3	15

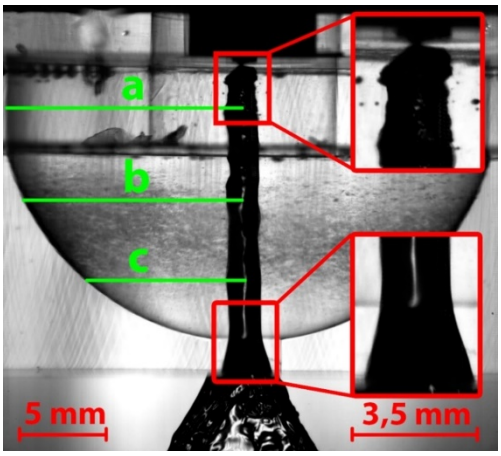

Figure 3. High-speed visualization, p-cymene, 1 MPa, Simplex, cross-section a, b and c placed 2.5, 8 and 13 mm from the top of the swirl chamber

3 Experimental and numerical setups

Following subchapters document the setups of the experimental approach using a high-speed camera and laser-Doppler anemometry (LDA) and the CFD simulations.

3.1 Experimental setup

The experiments were performed on the cold test bench at room temperature. A Photron SA-Z high-speed camera was used to document the spatial and temporal behaviour of the air core. The atomizer was illuminated by a background light using an LED panel. Three records were acquired at each operating regime; the first was a general image showing the whole atomizer while the other two observed the exit orifice and the top of the swirl chamber in close up, see Figure 3. The camera frame rate was 4,000 and 20,000 fps for the general image; the resolution was 1024 × 1024 px, and the shutter speed was set to 20 µs. The close-up records used a frame rate of 28,000 fps, resolution 768 × 904 px, and a shutter time of 10 µs. Mean and RMS images were calculated for each regime. The air core dimensions were captured by MATLAB code based on the Canny edge detector. The air core fluctuations were analysed using the Fast Fourier Transform (FFT) in the cross-section b. The FFT was applied to the time-resolved air core surface captured by the Canny edge detector. Another FFT was used on the average pixel intensities over a rectangle 3 × 3 px placed near the air core boundary to verify the previous FFT approach. The air core dimensions were measured at three cross-sections (a, b and c) over the swirl chamber and one cross-section at the tip of the exit orifice.

The LDA, a FlowExplorer (Dantec Dynamics A/S), was employed for the point-wise measurement of the velocity of individual particles inside the transparent atomizer. The swirl velocity component was measured in three cross-sections across the swirl chamber (see Figure 3 right). The axial distances from the top of the swirl chamber were 2.5, 8 and 13 mm for cross-sections a, b and c respectively, and 50, 38 and 25 measurement points were taken on each cross-section. The distance between two surrounding points was 0.25 mm. The LDA was configured in the backscatter mode. A built-in, diode-pumped solid-state laser generated a beam with 660 nm wavelength. The beam was split into two parallel beams with the power of 30 mW each. One of the beams was shifted by 80 MHz. A converging transmitting/receiving lens with 150 mm focal length was used to form an ellipsoidal measurement volume with the size of app. 0.1 × 0.1 × 0.8 mm. Dantec BSA P80 signal processor was used to process the measured signal. BSA flow software v5.20 was used to control the data acquisition and the following setting was used: Photomultiplier sensitivity 700 V, signal gain 20 dB, velocity centre 2.4 m/s, velocity span 4.8 m/s. The measurement was limited to 10,000 samples acquired or a 10-second acquisition duration at each measured point. A repeatability error based on three consequent measurements was less than 4%. The measuring volume position relative to the LDA positioning system had to be corrected due to the different refractive index of the atomizer body and the liquid as [35]:

$$S_2 = \frac{R}{1 + \frac{n_1}{n_2}\left(\frac{R}{n_1 S_1} - 1\right)} \quad (5)$$

,

where S_1 is the virtual distance of measurement volume from the atomizer wall, S_2 is the real distance of measurement volume, R is the diameter of the swirl chamber at measurement plane, n_1 and n_2 are the refractive indexes of PMMA and kerosene respectively. The measured velocity was multiplied by correction coefficient k_{vel} based on the simplified approach from [35] as:

$$k_{vel} = 1 + \left(\frac{n_1}{n_2} - 1\right)\frac{S_2}{R} \quad . \qquad (6)$$

The correction factor reached the maximum of 1.04 for kerosene at the atomizer axis. In positions close to the air-core, the raw velocity data were filtered since the strong noise was generated by the reflection from the air core surface. The filtration process seeks for the Gaussian distribution in the velocity histogram, and the mean velocity was calculated only from the data which satisfied the Gaussian distribution.

The flow tracer particles were SL75 e-spheres with a mean diameter of 45 μm. Their Stokes number, based on the swirl velocity and diameter of the swirl chamber, was less than 0.01 for each regime, which ensured a sufficiently small flow traceability error.

3.2 Numerical setup

Conservation of mass (continuity) and conservation of momentum (Navier–Stokes) equations were solved numerically using Ansys Fluent 17.2. The flow simulation was conducted as a transient 2D axisymmetric model. A Volume of Fluid (VOF) model with the geo-reconstruct scheme was used to capture the boundary of the air core. The 3D inlet boundary condition was set to conserve the mass flow rate in the radial direction and ensure the same angular momentum in the tangential direction. The pressure outlet boundary condition was applied on the outer boundaries with no-slip conditions applied on the wall boundaries. A laminar flow was assumed due to the low *Re* values inside the inlet ports, and also because inside the swirl chamber, the radial forces of the swirl tend to laminarise the flow [34]. The simulations were performed for both the original and scaled atomizers. The SR atomizer was simulated including a 4-mm long part of the spill-line geometry (see Figure 10 in section 4.3). The spill flow in the regime with SFR = 0.4 was set as a negative liquid source across the entire spill-line. It was not possible to set the pressure boundary condition to the spill-line wall as the solution was very unstable.

The all quad structured mesh with an average skewness of 0.058 and an average aspect ratio of 1.18 was created (Figure 4), and the mesh independence test was carried out for four different element base sizes in terms of C_D, SCA and the air core diameter (d_a) at the end of the exit orifice (d_o) in a dimensionless form as d_a/d_o (see Table 2). There was a significant difference between the meshes of 11,684 and 22,669 elements. This difference decreased with further increase in the number of elements, and the mesh with 46,765 elements was chosen as a good compromise between the accuracy and the calculation speed. Two sizes of an outflow area, which is an artificial area downstream of the atomizer outlet, were also tested. A calculation of four times larger outflow area revealed the same results as the original one, see results for meshes with 68,610 and 46,765 elements.

Table 2. Mesh independence test

Number of elements	C_D [–]	d_a/d_o [–]	SCA [deg]
11,684	0.392	0.655	58
22,669	0.365	0.707	58
46,765	0.358	0.710	57
68,610*	0.359	0.710	57
90,684	0.356	0.711	56

*The base size of the elements was the same as in the case of 46,765 elements. The outflow area was four times larger.

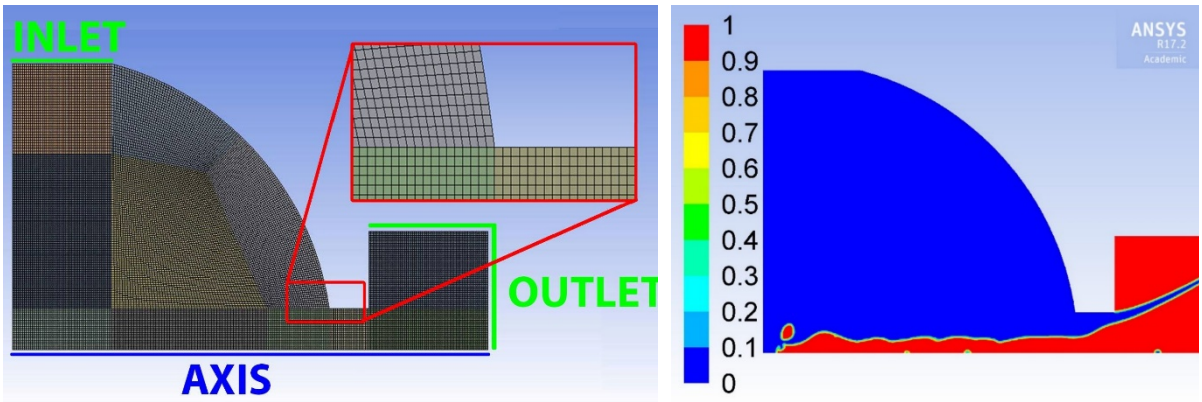

Figure 4. Left: Numerical domain and its mesh. Right: Typical results obtained with the wavy surface of the air core, phase distribution: 1 = air, 0 = liquid.

4 Results and discussion

The air core shape and stability play a key role in the formation of the liquid sheet at the discharge orifice. A description of the air core dynamics is based on high-speed image records and numerical simulations. The discharge parameters are discussed in terms of C_D and SCA. The measured swirl velocity profiles served for consequent validation of the numerical simulations.

4.1 Air core shape and spray cone angle

In a comparative manner, the high-speed records with both kerosene and p-cymene as the working liquid are shown in Figure 5. For the kerosene image, there are darker regions towards the edge of the swirl chamber. This is caused by light refraction at the swirl chamber wall. It is not evident in the atomizer centre due to the small relative curvature. This is solved using the liquid with the same refractive index as the atomizer body which can be seen for the results of p-cymene.

The air core was fully developed in the case of all the Simplex atomizers. It was cylindrically shaped and increased in its diameter inside the exit orifice; such behaviour was also described by other authors [16, 17, 28]. The dimensionless diameter of the air core in the exit orifice was $d_a/d_o = 0.72 \pm 0.02$ for all the inlet pressures and both liquids with no evident correlations to *Re*. Inside the swirl chamber, $d_a/d_o = 0.47 \pm 0.03$ and it was also almost independent of *Re*. Both findings are in accordance with other authors [16, 36, 37] who reported the independent air core size for high *Re* regimes, while Halder and Som [16] found a slightly increasing air core diameter with *Re*. Instabilities, in the form of air core fluctuations, both in the axial and radial direction (Figure **6**), were observed at the top of the swirl chamber. These fluctuations are linked with the wavy structure on the air core surface. The frequency of the surface waves $f = 32 \pm 4$ Hz was estimated using the FFT analysis of images for the Simplex atomizer with p-cymene at $Re = 1021$. A similar analysis was reported by Sumer et al. [30] who used a similarly sized atomizer, but with the velocity in the inlet ports approximately ten times higher; they found wave frequencies of $f = 273$ Hz. Chinn et al. in [38] studied the surface waves on the air core and described three distinctive types of surface waves: helical striations, stationary waves and random ripples. They noted that the stationary waves were responsible for changes in the liquid sheet thickness. The same phenomenon was also evident in our records. The helical striations, which are caused by finite number of the inlet ports, were not observed here.

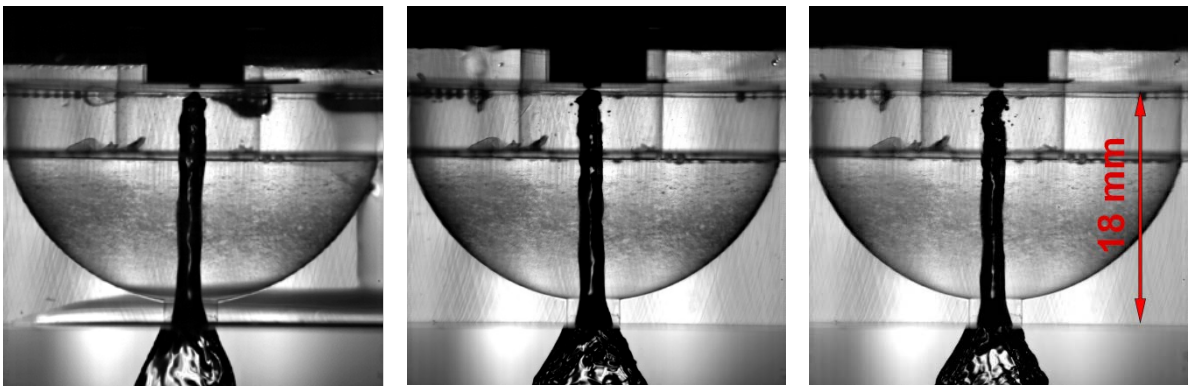

Figure 5. Simplex atomizer, Top: Kerosene, Bottom: P-cymene. From left to right: flow regime equivalent to 0.5 MPa (*Re* = 755), equivalent to 1 MPa (*Re* = 1021), equivalent to 1.5 MPa (*Re* = 1252).

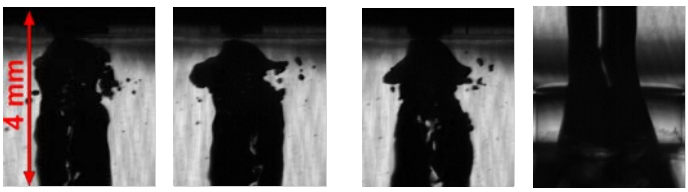

Figure 6. Simplex, p-cymene, *Re* = 1021, the temporal evolution of the air core tip. Right: the detail on the exit orifice.

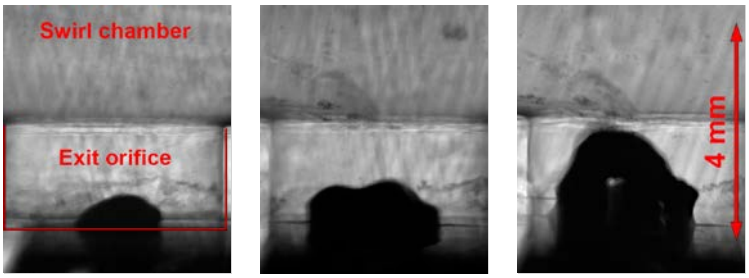

Figure 7. The exit orifice in detail. SR atomizer, flow regime from left to right: equivalent to 0.5 MPa (*Re* = 1075), equivalent to 1 MPa (*Re* = 1431), equivalent to 1.5 MPa (*Re* = 1731).

The situation changed dramatically when the SR atomizer was used. The air core is no longer present in the swirl chamber, and the spray becomes unstable, even for the highest *Re* values. Only fragments of the core are visible inside the exit orifice (see Figure 7). The air core was unstable and strongly fluctuating and it even occasionally disappeared. The SCA was fluctuating between 49 and 88 deg with a frequency in the range of 10–20 Hz with no evident correlation to the air core behaviour. This was observed for all regimes with the spill-line closed.

With increasing spilled flow rate the swirling momentum increases with respect to the axial momentum and the flow character changes. The standard mean deviation of SCA features a high value up to spill-to-feed ratio (SFR) 0.15 as shown in Figure 8, which corresponds to strong fluctuations. With further increase in SFR, the fluctuations reduce, and the SCA correlates with SFR as $SCA = 62.1+23.8\times SFR^{1.5}$ (see the correlation line in Figure 8). However, at high SFRs, where the injection flow rate is very low, the fluctuations of SCA become stronger again. The air core is limited to the exit orifice even at SFR 0.4; however, for SFRs higher than 0.15, it is stable enough not to decay. In the relatively narrow range of SFR 0.4–0.65, the air core extends into the swirl chamber. With further increase in SFR, the air core penetrates through the spill orifice so it was not possible to make a further measurement of its length. It is evident that the spray stability is linked to the air core stability within the exit orifice, but it is not necessary to provide a fully developed air core across the entire swirl chamber height to ensure a stable spray. The standard mean deviation of SCA for Simplex and SR atomizers at SFR 0.3–0.4 are approximately equal even if the air core is not fully developed as in the case of SR atomizer.

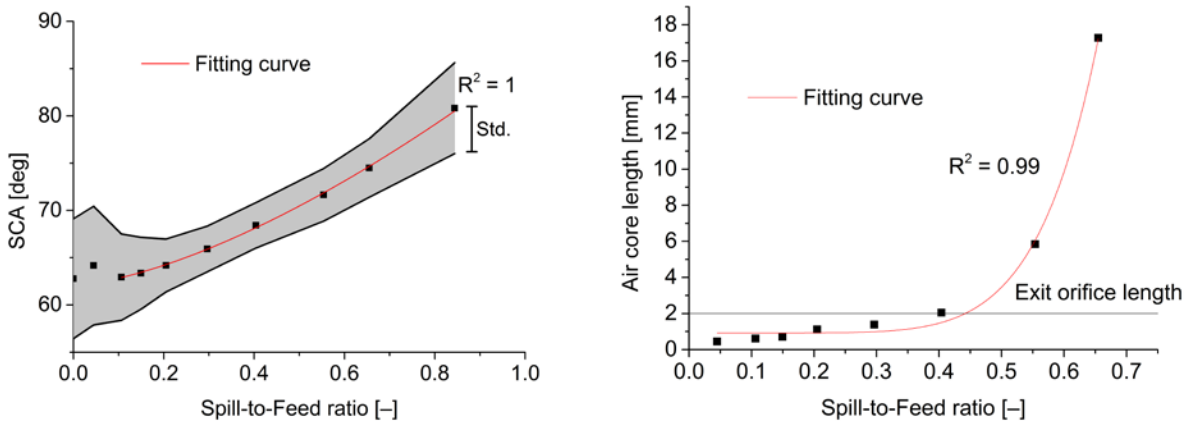

Figure 8 SCA (left) and air core length (right) in dependence on SFR

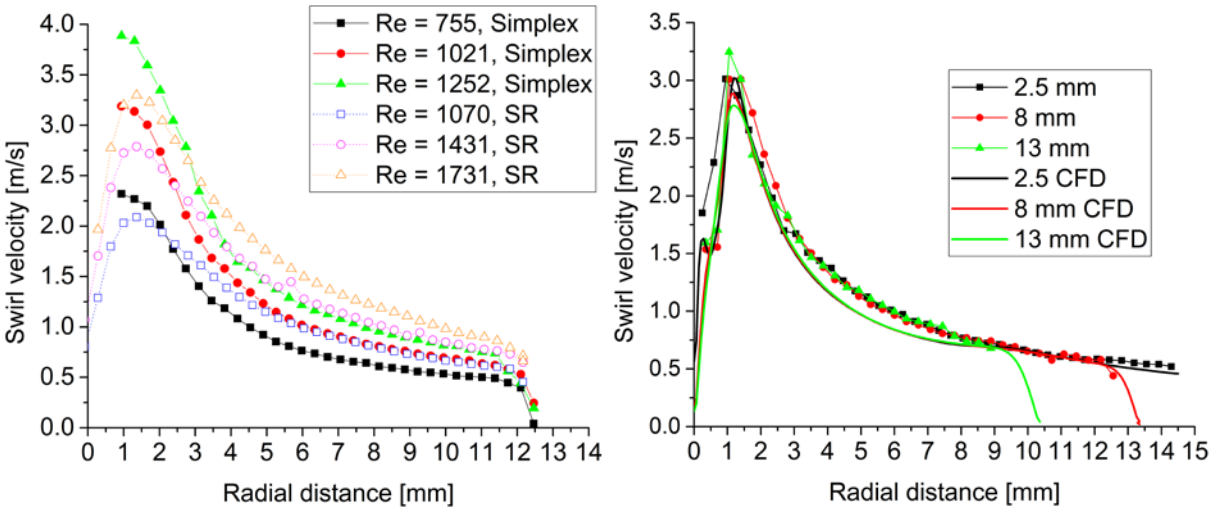

Figure 9. Swirl velocity profiles from Simplex and SR atomizer; left: kerosene, cross-section b (8 mm from the top), right: comparison of numerical and experimental profiles of swirl velocity, kerosene, Simplex, *Re* = 1021.

4.2 Velocity profile inside the swirl chamber

The measured profiles of the swirl velocity (Figure 9, left) show a disparity between the Simplex and SR atomizers. The velocity profile for the Simplex version features a relatively sharp maximum near the air core interface, which is typical for a Rankine vortex. The central air core behaves like a solid body of the vortex core. In the outer region, a potential vortex distribution can be found. Several authors published a similar velocity profile [39, 40]. The swirl velocities are almost identical for all axial distances in both the experiment and simulation (see Figure 9, right). This is in agreement with the inviscid theory where the swirl velocity depends on the inlet velocity and radial distance from the axis of the swirl chamber out to the mid-point of inlet ports.

In contrast to the Simplex atomizer, the SR type shows a flatter peak with lower velocity maximum at similar *Re* values. No air core forms and so the atomizer centre is filled with the viscous liquid. This causes a viscous decay of the velocity and the velocity maximum is thus lower, and its peak is flatter.

The trends in the swirl velocity profiles were almost equivalent between experiments and simulations. The simulation slightly underestimates the velocity magnitude at the air core boundary. Similar studies were carried out by Hansen and Madsen [31, 39] who conducted both experimental and 3D computational studies of a large-scale PS atomizer. Their earlier study [39] showed that the 3D numerical simulation significantly underestimated the swirl velocity magnitude. In their following work [31], the numerical grid was modified and the inlet tangential ports were properly modelled which reduced the differences between the experimental and numerical velocity magnitude. This is in contrast to our case where the simple 2D simulation was able to closely predict the swirl velocity even if the inlet ports were replaced by an annular slot.

The numerical simulation reveals some secondary flow effects in the swirl chamber. Görtler vortices can be seen in the near-wall region for both the Simplex and SR atomizers (see the path lines in Figure 10). A similar behaviour was described in [41].

4.3 Discharge characteristics

Both, the original and scaled Simplex atomizers have virtually the same C_D (see Table 1). This is expected as they have the same atomizer constant *k*, operating liquid, and *Re*. However, the SR version shows some disparity between the original and scaled atomizer in the C_D. The scaled atomizer featured a noticeably smaller C_D. This behaviour was attributed to the diameter of the outflow area behind the spill orifice, which was not sized proportionally in the transparent model according to the original atomizer.

The numerical results of Simplex atomizer, when compared with the experiments in terms of global characteristics (C_D and SCA), give a very good agreement (Table 3). The most significant difference was found in the case of low *Re* values where the numerical solution overestimated the C_D by 5%. An increase in *Re* results in a slight decrease in C_D for both the experimental and numerical solutions. The results based on the inviscid theory are dependent only on the atomizer geometry and were calculated in accordance to Chinn [8, 9]. The C_D was underestimated by about 15%, and the spray cone angle was overestimated by about 35 to 65% depending on the equation used. These results can be expected as, in the real viscous flow; the friction forces cause a decrease in angular momentum. Due to this, the air-core is smaller in diameter, which causes an increase in flow cross-section over the exit orifice, and thus the C_D is increased. Similarly, the SCA is smaller as the angular momentum is decreased. Rizk and Lefebvre [10] published modified correlations for C_D and SCA which show a fair agreement with our experimental and numerical results (see Table 13). However, they did not consider the effect of *Re* in their correlation.

In all the numerical simulations of the Simplex atomizers, the wavy interface between the liquid and gas phases was unsteady, see Figure 4, right. The frequency of the surface wave in the centre of the swirl chamber was, in the case of p-cymene, for $Re = 1021$ app. 25 ±4 Hz, which agrees well with $f = 32 \pm 4$ Hz as in the experiment. However, the fluctuations of the air core tip were overestimated in the simulation as the air core was periodically detaching from the rear wall of the swirl chamber (see Figure 4).

The unstable behaviour of the SR atomizer was captured well by the simulation. The air core was limited to the exit orifice area in a similar way to the experiments (see Figure 10 and Table 4). However, the dimension of the spill-line outflow area affected the numerical results. A larger outflow area, as shown in Figure 10, increased the instabilities of the air core and C_D. This is in agreement with Table 1 where the original atomizer had a relatively large spill outflow area compared to the transparent atomizer. The analysis of the velocity fields inside the spill orifice (see Figure 10) reveals a recirculation zone inside the spill-line. The liquid flows in both directions thought the spill orifice as it is drawn back into the swirl chamber due to the low-pressure regime in the swirl chamber centre. This flow nature was also observed in the high-speed records. The off-axis replacement of the spill orifice will change the flow behaviour as the pressure distribution across the spill orifice will be uniform; thus, the backflow will be unfeasible.

It shows that our former hypothesis, as regards to a periodically decaying air core as based on the external observation of the original atomizer spray [22], was misleading; the air core is not formed at all. This is consistent with the fact that the atomizers with the off-axis spill-orifice provide a stable spray under all regimes [22] while, under the regimes with closed spill-line, they behave in the same way as the Simplex type.

Table 3 Comparison of numerical and experimental results of the Simplex atomizer

	***Re* = 755**		***Re* = 1021**		***Re* = 1252**			
	Num.	**Exp.**	**Num.**	**Exp.**	**Num.**	**Exp.**	**Inviscid** [8, 9]	**Rizk** [10]
C_D **[–]**	0.410	0.387	0.359	0.369	0.366	0.365	0.312	0.359
SCA [deg]	56.7	58.6	58	59.5	58.7	60.3	80–100	51.6*
d_a/d_o **[–]**	0.62	0.70	0.71	0.71	0.71	0.71	0.7–0.8	–

**Re* = 1021

Table 4 Comparison of numerical and experimental results of SR atomizer

	SR, *Re* = 1431, SFR 0			SR, *Re* = 1676, SFR 0.4	
	Exp.	**Spill A**	**Spill B**	**Exp.**	**Num.**
C_D [–]	0.519	0.448	0.460	0.378	0.342
SCA [deg]	62.8	57.6	58.2	68	60
d_a/d_o [–]	Decaying	0.45	Decaying	0.56	0.57

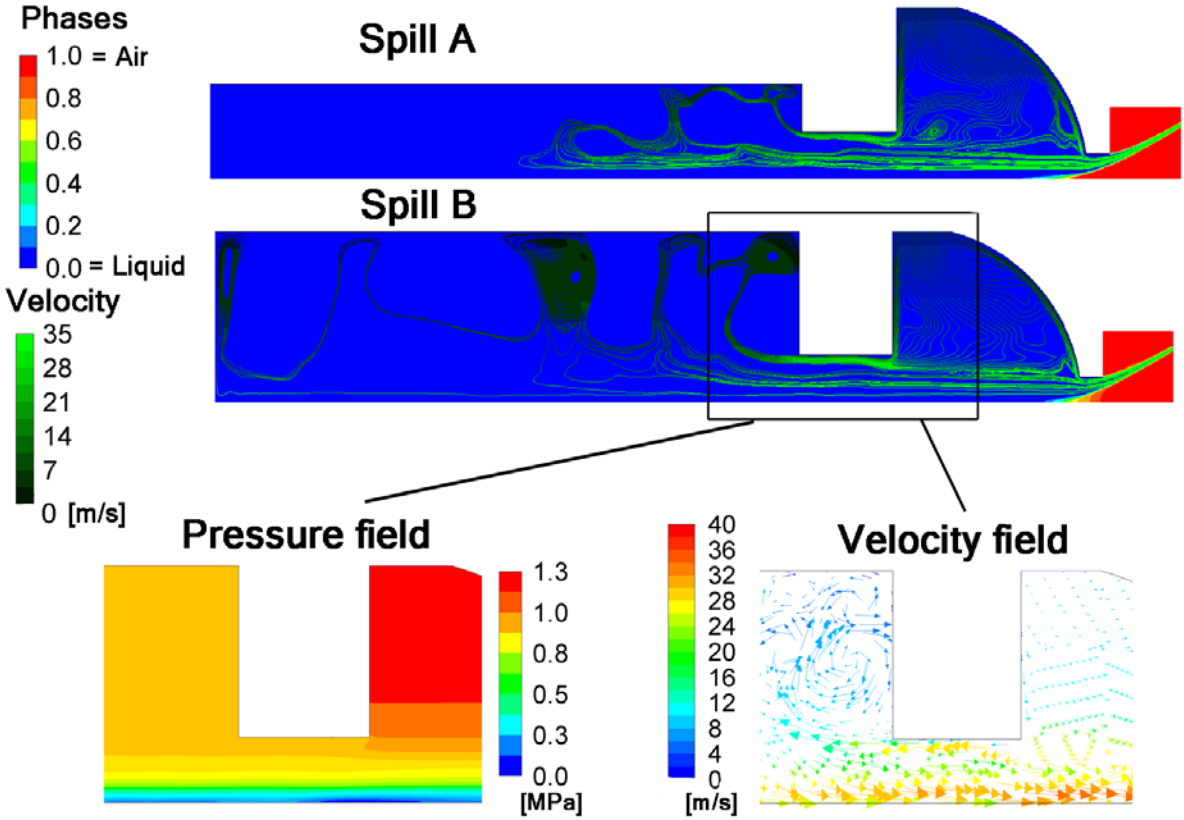

Figure 10 Spill A and Spill B**:** Mean phase distributions and path lines**,** different spill-line geometry. Bottom: a detail of the spill-line: A) pressure field, B) 2D velocity vector field (vector count reduced 50 times).

5 Conclusions

The discharge and internal flow characteristics of Simplex and SR atomizer, with a central SR orifice, were examined both experimentally and numerically. The numerical results were validated against the results obtained from the high-speed images and point-wise LDA measurements.

The Simplex atomizer featured a stable, cylindrically shaped air core. Its diameter was found independent of *Re* under the measured range of operating conditions.

The numerical simulation, assuming a laminar flow, was able to closely predict the global characteristics (C_D, SCA). The trends and magnitude in mean swirl velocity were both well captured. Unstable waves were observed on the surface of the air core using high-speed imaging and were also captured by the numerical simulation.

The SR atomizer with axially placed spill orifice produced an internal flow without the air core; therefore, the spray fluctuated strongly. A recirculation zone was found inside the spill-line and the liquid flows through the spill orifice in both directions. The velocity profiles showed lower and flatter peak values in comparison to the Simplex atomizer at similar *Re* values. Spill orifices placed off-axis will stabilize the internal flow.

This study provides the primary groundwork for the internal flow analysis of SR atomizers. Further investigations including a more realistic 3D computational model, several different

arrangements of the spill orifice and a range of SFRs will follow. The numerical approach proved to be a strong tool for further atomizer design.

6 Acknowledgements

This work has been supported by the project No. GA15-09040S funded by the Czech Science Foundation and the project no. CZ.1.05/2.1.00/19.0397, NETME Centre TechUp with the financial support from the Ministry of Education, Youth and Sports of the Czech Republic under the "National Sustainability Programme I" and project Reg. No. FSI-S-17-4444 funded by the Brno University of Technology.

7 Nomenclature

A	area [mm^2]
b	width [mm]
C_D	discharge coefficient [–]
d	diameter [m]
f	frequency [–]
k_{vel}	correction factor [–]
Fr	Froude number [–]
h	height [mm]
$\dot{m}$	mass flow rate [kg/s]
n_1	refractive index of PMMA
n_2	refractive index of liquid
Q	volumetric flow rate [–]
r	radial distance [mm]
R	radius of swirl chamber at measurement plane [mm]
Re	Reynolds number [–]
SCA	spray cone angle [deg]
SFR	Spill-to-Feed ratio
S_1	virtual distance of the measurement volume from the atomizer wall [mm]
S_2	real distance of the measurement volume [mm]
S_o	Swirl number [–]

Greek characters

Δp	pressure drop at the nozzle [MPa]
μ	dynamic viscosity [kg/(m·s)]
ρ	density [kg/m^3]
σ	liquid/gas surface tension [kg/s^2]

Subscripts and Superscripts

l	atomized liquid
o	exit orifice
s	swirl chamber
p	inlet port
a	air core

8 References

[1] Lefebvre, A. H., 1989, Atomization and sprays, Hemisphere Pub. Corp., New York.
[2] Lefebvre, A. H., and Ballal, D. R., 2010, "Gas turbine combustion," Taylor & Francis
[3] Rizk, N., and Lefebvre, A., 1985, "Drop-size distribution characteristics of spill-return atomizers," Journal of Propulsion and Power, 1(1), pp. 16-22.
[4] Carey, F. H., 1954, "The Development of the Spill Flow Burner and Its Control System for Gas Turbine Engines," Journal of the Royal Aeronautical Society, 58, pp. 737-753.
[5] Kapitaniak, A., 1967, "The Influence of Chosen Construction Parameters on the Performance of Spill-Control Pressure-Jet Atomizers," Journal of the Institute of Fuel, pp. 24-35.
[6] Nasr, G., Yule, A., Stewart, J., Whitehead, A., and Hughes, T., 2011, "A new fine spray, low flowrate, spill-return swirl atomizer," Proceedings of the Institution of Mechanical Engineers, Part C: Journal of Mechanical Engineering Science, 225(4), pp. 897-908.
[7] Taylor, G. I., 1948, "The Mechanics of Swirl Atomizers," International Congress of Applied MechanicsLondon.
[8] Chinn, J. J., 2009, "An appraisal of swirl atomizer inviscid flow analysis, Part 1: The principle of maximum flow for a swirl atomizer and its use in the exposition and comparison of early flow analyses," Atomization and Sprays, 19(3).
[9] Chinn, J. J., 2009, "An appraisal of swirl atomizer inviscid flow analysis, part 2: inviscid spray cone angle analysis and comparison of inviscid methods with experimental results for discharge coefficient, air core radius, and spray cone angle," Atomization and Sprays, 19(3).
[10] Rizk, N. K., and Lefebvre, A. H., 1985, "Internal flow characteristics of simplex swirl atomizers," Journal of Propulsion and Power, 1(3), pp. 193-199.
[11] Jones, A., 1982, "Design optimization of a large pressure-jet atomizer for power plant," Proceedings of the Second International Conference on Liquid Atomization and Spray Systems.
[12] Ballester, J., and Dopazo, C., 1994, "Discharge coefficient and spray angle measurements for small pressure-swirl nozzles," Atomization and sprays, 4(3).
[13] Benjamin, M., Mansour, A., Samant, U., Jha, S., Liao, Y., Harris, T., and Jeng, S., "Film thickness, droplet size measurements and correlations for large pressure-swirl atomizers," Proc. ASME 1998 International Gas Turbine and Aeroengine Congress and Exhibition, American Society of Mechanical Engineers, p. 8.
[14] Wimmer, E., and Brenn, G., 2013, "Viscous flow through the swirl chamber of a pressure-swirl atomizer," International Journal of Multiphase Flow.

[15] Malý, M., Janáčková, L., Jedelský, J., and Jícha, M., 2016, "Impact of alternative fuel rheology on spraying process of small pressure-swirl atomizer," AIP Conference Proceedings, AIP Publishing.
[16] Halder, M., Dash, S., and Som, S., 2002, "Initiation of air core in a simplex nozzle and the effects of operating and geometrical parameters on its shape and size," Experimental thermal and fluid science, 26(8), pp. 871-878.
[17] Lee, E. J., Oh, S. Y., Kim, H. Y., James, S. C., and Yoon, S. S., 2010, "Measuring air core characteristics of a pressure-swirl atomizer via a transparent acrylic nozzle at various Reynolds numbers," Experimental thermal and fluid science, 34(8), pp. 1475-1483.
[18] Kim, S., Khil, T., Kim, D., and Yoon, Y., 2009, "Effect of geometric parameters on the liquid film thickness and air core formation in a swirl injector," Measurement Science and Technology, 20(1).
[19] Moon, S., Abo-Serie, E., and Bae, C., 2009, "Air flow and pressure inside a pressure-swirl spray and their effects on spray development," Experimental Thermal and Fluid Science, 33(2), pp. 222-231.
[20] Park, S. H., and Shin, H. D., 1993, "Measurements of entrainment characteristics of swirling jets," International Journal of Heat and Mass Transfer, 36(16), pp. 4009-4018.
[21] Khavkin, Y., 2004, The Theory and Practice of Swirl Atomizers, Taylor & Francis.
[22] Jedelsky, J., Malý, M., Janáčková, L., and Jícha, M., 2016, "Effect of Geometric Factors on Spray Characteristics and Stability for Small Spill-Return Pressure-Swirl Atomizers," ILASS 2016Brighton, p. 12.
[23] Slowik, G., and Kohlmann, J., 2006, "A swirl controlled hollow cone nozzle and its technical applications," ICLASS06.
[24] Horvay, M., and Leuckel, W., 1985, "LDA-measurements of liquid swirl flow in converging swirl chambers with tangential inlets," 2nd International Symposium on Applications of Laser Anemometry to Fluid Mechanics, p. 11.
[25] Kraemer, M., Horvay, M., Loeffler-Mang, M., and Leuckel, W., 1988, "Velocity profile measurements within swirl pressure-jet nozzles using LDA," Laser Anemometry-Advances and Applications, pp. 141-152.
[26] Yule, A. J., and Chinn, J., 1994, "Swirl atomizer flow: classical inviscid theory revisited," ICLASS-94, Rouen, France.
[27] Yule, A., and Chinn, J., 1997, "Pressure swirl atomizer internal flow and performance," ILASS, Americas, pp. 205-209.
[28] Amini, G., 2016, "Liquid flow in a simplex swirl nozzle," International Journal of Multiphase Flow, 79, pp. 225-235.
[29] Mandal, A., Jog, M., Xue, J., and Ibrahim, A., 2008, "Flow of power-law fluids in simplex atomizers," International journal of heat and fluid flow, 29(5), pp. 1494-1503.
[30] Sumer, B., Erkan, N., Uzol, O., and Tuncer, I., 2012, "Experimental and Numerical Investigation of a Pressure Swirl Atomizer," ICLASS.
[31] Madsen, J., Hjertager, B. H., and Solberg, T., 2004, "Numerical simulation of internal flow in a large-scale pressure-swirl atomizer," ILASS, pp. 183-188.
[32] Abbasi Baharanchi, A., Nordin Darus, A., Ansari, M., and Abbasi Baharanchi, E., 2012, "An Optimum Method of Capturing Interface and a Threshold Weber Number for Inclusion of Surface Tension Force in Simulation of Nozzle Internal Flow in Pressure Swirl Atomizers," (ASME International Mechanical Engineering Congress and Exposition), p. 12.
[33] Durdina, L., Jedelsky, J., and Jicha, M., 2014, "Investigation and comparison of spray characteristics of pressure-swirl atomizers for a small-sized aircraft turbine engine," International Journal of Heat and Mass Transfer, 78(0), pp. 892-900.
[34] Chinn, J. J., 2008, "The numerics of the swirl atomizer," ILASS.
[35] Zhang, Z., 2010, LDA Application Methods: Laser Doppler Anemometry for Fluid Dynamics, Springer.
[36] Datta, A., and Som, S., 2000, "Numerical prediction of air core diameter, coefficient of discharge and spray cone angle of a swirl spray pressure nozzle," International journal of heat and fluid flow, 21(4), pp. 412-419.
[37] Moon, S., Abo-Serie, E., and Bae, C., 2010, "Liquid film thickness inside the high pressure swirl injectors: Real scale measurement and evaluation of analytical equations," Experimental Thermal and Fluid Science, 34(2), pp. 113-121.
[38] Chinn, J., Cooper, D., Yule, A., and Nasr, G., 2015, "Stationary rotary force waves on the liquid–air core interface of a swirl atomizer," Heat and Mass Transfer, pp. 1-14.
[39] Hansen, K., Madsen, J., Trinh, C., Ibsen, C., Solberg, T., and Hjertager, B., 2002, "A computational and experimental study of the internal flow in a scaled pressure-swirl atomizer," Zaragoza, 9, p. 11.
[40] Horvay, M., and Leuckel, W., 1986, "Experimental and theoretical investigation of swirl nozzles for pressure-jet atomization," German chemical engineering, 9(5), pp. 276-283.
[41] Cooper, D., Yule, A., and Chinn, J., 1999, "Experimental measurements and computational predictions of the internal flow field in a pressure swirl atomizer," ILASS 1999.